Computational Approach to Nuclear Magnetic Resonance in 1-Alkyl-3-methylimidazolium Ionic Liquids

Jose Palomar,* Victor R. Ferro, Miguel A. Gilarranz, and Juan J. Rodriguez

Sección de Ingeniería Química, Dpt. Química Física Aplicada, Universidad Autónoma de Madrid, Cantoblanco, 28049 Madrid, Spain

Received: June 7, 2006; In Final Form: October 10, 2006

A quantum-chemical computational approach to accurately predict the nuclear magnetic resonance (NMR) properties of 1-alkyl-3-methylimidazolium ionic liquids has been performed by the gauge-including atomic orbitals method at the B3LYP/6-31++G** level using different simulated ionic liquid environments. The first molecular model chosen to describe the ionic liquid system includes the gas-phase optimized structures of ion pairs and separated ions of a series of imidazolium salts containing methyl, butyl, and octyl substituents and PF_6^-, BF_4^-, and Br^- anions. In addition, a continuum polarizable model of solvation has been applied to predict the effects of the medium polarity on the molecular properties of 1,3-dimethylimidazolium hexafluorophosphate ($MmimPF_6$). Furthermore, the specific acidic and basic solute−solvent interactions have been simulated by a discrete solvation model based on molecular clusters formed by $MmimPF_6$ species and a discrete number of water molecules. The computational prediction of the NMR spectra allows a consistent interpretation of the dispersed experimental evidence in the literature. The following are main contributions of this work: (a) Theoretical results state the presence of a chemical equilibrium between ion-pair aggregates and solvent-separated counterions of 1-alkyl-3-methylimidazolium salts which is tuned by the solvent environment; thus, strong specific (acidic and basic) and nonspecific (polarity and polarizability) solvent interactions are predicted favoring the dissociated ionic species. (b) The calculated ^1H and ^{13}C NMR properties of these ionic liquids are revealed as highly dependent on the nature of solute−solvent interactions. Thus, the chemical shift of the hydrogen atom in position two of the imidazolium ring is deviated to high values by the specific interactions with water molecules, whereas nonspecific interaction with water (as a solvent) affects, in the opposite direction, this ^1H NMR parameter. (c) Last, current calculations support the presence of hydrogen bonding between counterions, suggesting the importance of this interaction in the properties of the solvent in the 1-alkyl-3-methylimidazolium ionic liquids.

1. Introduction

Quantum-chemical methods have been largely applied as a valuable tool to the analysis of numerous spectroscopic data.[1] Nowadays, as a consequence of the development of ab initio computations, rapid and reliable predictions of a wide variety of spectroscopic parameters for medium-sized molecules are becoming routine.[2] Also, the domain of computational applications is becoming amenable for a larger part of the chemical community. As a result, the size and nature of the chemical systems studied by quantum-chemical calculations have been significantly increased in the last years.[3]

A field of increasing interest to chemists and chemical engineers is the room-temperature ionic liquids (RTIL). Ionic liquids have gained popularity as suitable green solvents because of their unique properties: negligible vapor pressure, high thermal and chemical stability, wide liquid-state range, and high solvent capacity.[4,5] Thus, the application of these novel solvents to organic synthesis, organometallic catalysis, electrochemistry, biocatalysis, material science, and separation processes is being extensively investigated.[6−8] In particular, the family of ionic liquids based on 1-alkyl-3-methylimidazolium salts has received special attention because their solvent properties are readily tuned through the selection of either the cationic or the anionic component for a specific application.[9] As a result, the exponentially growing research has led to a deeper understanding of RTIL properties at a molecular level by several analytical techniques.[10]

Nuclear magnetic resonance (NMR) has been one of the most widely applied spectroscopies to investigations of 1-alkyl-3-methylimidazolium ionic liquids (see Scheme 1).[11−34] On the one hand, ^1H NMR measurements are being routinely performed to confirm the cation structure and to analyze the purity of the ionic liquids synthesized. To our knowledge, first assignments of the ^1H NMR spectra of this family of ionic liquids were performed by Seddon et al.,[11] Grätzel et al.,[12] and Armstrong et al.[13] On the other hand, the main aim of several NMR studies on ionic liquids has been to obtain a better understanding of the nature of the interaction between cation and anion or between the solvent molecules and the ionic liquid species in solution. As a matter of fact, the significant dependence of the ^1H and ^{13}C NMR chemical shifts of these imidazolium salts on anion, alkyl chain, or solvent environments has been repeatedly reported in References and Notes.[11−25] In this way, Carper et al. have reported several ^{13}C NMR relaxation rate studies on imidazolium-based ionic liquids providing valuable information concerning the reorientational dynamics and molecular interactions that occur in the liquid state.[26−32] Another NMR application recently established by Giernoth et al. describes the use of

* Corresponding author. E-mail: pepe.palomar@uam.es.

10.1021/jp063527s CCC: $37.00
Published on Web 12/13/2006

SCHEME 1

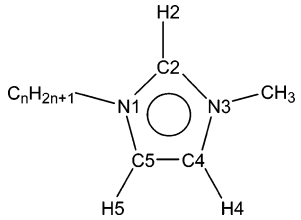

ionic liquid solvents for in situ studies of reactions by high-resolution NMR measurements.[33,34]

Unfortunately, the available reports on NMR investigations of ionic liquids showed confusing and even contradictory analysis of the experimental data. For example, on the basis of NMR evidence, the question of the existence of hydrogen-bonding interaction involving both the cation and the anion of ionic liquids has been addressed. Thus, Suarez et al.[14] presented the ^{1}H and ^{13}C NMR spectra of the neat ionic liquids 1-butyl-3-methylimidazolium tetrafluoroborate ($BmimBF_4$) and 1-butyl-3-methylimidazolium hexafluorophosphate ($BmimPF_6$), attributing the high chemical shifts of imidazolium protons to a hydrogen bond with these anions. In contrast, Holbrey and Seddon[15] did not find unambiguous ^{1}H NMR evidence of hydrogen bonding in the liquid phase for 1-alkyl-3-methylimidazolium tetrafluoroborate salts ($C_n mimBF_4$, $n = 0-18$) since the chemical shift values of C2−H2 protons of these ionic liquids in a deuterated propanone solution are all similar. In contrast, Wang et al.[17] explained the temperature dependence of ^{11}B and ^{13}C relaxation rates of BF_4^- and the C2 atom in neat 1-ethyl-3-methylimidazolium tetrafluoroborate ($EmimBF_4$) as a consequence of hydrogen bonding [C2−H2···F] between counterions. Furthermore, on the basis of nuclear Overhauser enhancement (NOE) experiments, Mele et al.[19] proposed the existence of tight ion pairs in pure $BmimBF_4$, in which the imidazolium protons are hydrogen bonded to the F atoms of the anion. Reports by Carper et al. on ^{13}C NMR relaxation rates in this family of ionic liquids also support the occurrence of hydrogen bonding between the imidazolium alkyl groups and the anions.[26−28]

The effect of the anion and the solvent environment on the NMR chemical shift values of 1-alkyl-3-methylimidazolium salts has also been a subject of discussion in References and Notes. An earlier work by Grätzel et al.[12] showed that, for a series of these ionic liquids diluted in acetone-d_6 at identical concentrations, the ^{1}H chemical shifts of the ring protons increase with the increasing anion basicity. However, the analysis of the obtained NMR data clearly shows that this behavior only occurs at low concentrations. At a higher concentration range, ^{1}H chemical shifts behave in the opposite direction, diminishing their values with the basicity of the anion. In addition, the ionic liquid concentration initially increases the ^{1}H NMR chemical shifts but subsequently may diminish their values at higher ionic liquid concentrations. The authors justified these results in terms of two effects: H-bonding leads to a higher chemical shift, but ring stacking leads to a lower chemical shift. On the other hand, Seddon et al.[16] revealed that the presence of a chloride impurity in pure $BmimBF_4$ and $BmimPF_6$ causes the C2−H2 chemical shift to move to a lower field. To a minor extent, this downfield shift was also observed in the signals of H4 and H5 protons. These NMR results were related to an increase in the cohesive forces via hydrogen bonding between the chloride anion and the protons of the imidazolium ring. In another solvent-effect study, Headley and Jackson[18] found a much broader chemical shift variation of the acidic H2 atoms than with the H4 and H5 atoms for $BmimBF_4$ and $BmimPF_6$ with the solvent nature, which was attributed to a more intimate interaction of the C2−H2 group with the anion. In contrast, Lin et al.[20] reported an extensive NMR study of a series of BF_4^- and PF_6^- methylimidazolium salts dissolved in high-polar solvents and concluded that the ^{1}H and ^{13}C chemical shifts were not influenced much by the variation in the type of solvents, the concentration, or even the length of the alkyl group in the ring.

Another interesting subject for analysis in NMR studies on ionic liquids is the possibility of chemical equilibrium between discrete ion pairs and individual ions in solution or those in ionic liquid media. Thus, on the basis of NMR measurements, Suarez et al.[14] proposed that the pure $BmimPF_6$ and $BmimBF_4$ behave in a quasi-molecular manner below 353 and 279 K, respectively, but at higher temperatures, they are composed of cations and anions in an extended hydrogen-bonded network. Consistent with previous results, Wang et al.[17] found NMR evidence of a phase change of the neat $EmimBF_4$ compound in the vicinity of 333 K. Concerning the experimental NMR evidence of different ionic liquid species in solution, Holbrey and Seddon[15] reported, in an earlier study, the presence of new ^{1}H NMR signals for tetrafluoroborate salts dissolved in trichloromethane (but not in solvents with higher polarity) which were assigned to a clathrate formation between the relatively acidic proton of the solvent and the BF_4^- anion. However, Hoffman and Tubbs[21] showed that the ionic liquid 1-ethyl-3-methylimidazolium bis(trifyl)imide (EmimTfN) clearly presents two resonance sets in the ^{1}H NMR spectrum whose intensities depend on the dielectric constant of the solvent media. The authors explained this result by the existence of an equilibrium between the freely dissolved ions and the ion-pair aggregates. As a consequence, the hypothesis of the formation of clathrates in diluted ionic liquids exposed by Holbrey and Seddon[15] seemed to be refuted. In this sense, Lin et al.[20] concluded, on the basis of ^{1}H and ^{13}C NMR measurements, that the ionic liquids formed by the 1-alkyl-3-methylimidazolium cation and the BF_4^- or PF_6^- anion are completely dissociated into individual ions in high-polar solvents. In addition, Mele et al.[19] suggested that, on the basis of NOE and rotating-frame Overhauser enhancement (ROE) spectroscopy experiments, the presence of small amounts of water replaces progressively the C−H···F interactions. New hydrogen bonds are detected involving solvent molecules as an acceptor toward the cation and as a donor toward the anion. In this way, Headley et al.,[22] on the basis of ^{1}H NMR spectra of imidazolium salts in different solvents, have recently proposed that there is a competition for the hydrogen bonding with the aromatic hydrogens of the cation for the solvent molecules and the anions.

In summary, it appears very likely through NMR measurements that specific interactions between the cation and the anion occur for this family of ionic liquids. However, the phenomena that affect their chemical shifts are still not unambiguously assigned, in particular, with respect to the possible ionic liquid species present in a determined chemical environment. In this work, we perform an extended theoretical analysis of 1-alkyl-3-methylimidazolium ionic liquids on the basis of quantum-chemical methods to predict their NMR properties in different molecular environments. We will use current computational approaches with the main aim of shedding some light on the complex behavior of NMR properties indicated in References and Notes.

To date, quantum-chemical calculations on imidazolium-based salts have successfully been applied to predict the infrared and Raman spectra of the neat and in-solution compounds,[35−37]

SCHEME 2

$$(C^+)_{\text{gas-phase}} + (A^-)_{\text{gas-phase}} \leftrightarrow (CA)_{\text{gas-phase}} \qquad \Delta E = E_{IL} \qquad \text{Eq. 1}$$

$$(C^+)_{\text{PCM}} + (A^-)_{\text{PCM}} \leftrightarrow (CA)_{\text{PCM}} \qquad \Delta E = (E_{IL})_{solvated} \qquad \text{Eq. 2}$$

$$\left.\begin{array}{l} (C^+)\cdot(H_2O)_{n-1} + (A^-)\cdot(H_2O)_n \leftrightarrow (CA)\cdot(H_2O)_{2n-1} \\ \text{or} \\ (C^+)\cdot(H_2O)_n + (A^-)\cdot(H_2O)_n \leftrightarrow (CA)\cdot(H_2O)_{2n} \end{array}\right\} \quad \Delta E = (E_{IL})_{solvated} \qquad \text{Eqs. 3}$$

the thermodynamics of ionic liquid formation,[38,39] the location of the anion with respect to the imidazolium ring in ionic liquid crystals, and the existence of hydrogen-bonding interactions between counterions.[40−42] Most of these computational studies used density functional theory (DFT) in conjunction with gas-phase molecular models to simulate the ionic liquid system. However, in recent years, different theoretical approaches have been employed to evaluate the environmental effects on molecular properties. The polarizable continuum model (PCM), as a valuable quantum-chemical tool, has simulated a condensed phase in the case of low-polar solvents.[43] However, these implicit solvation models may fail to correctly reproduce the effects of highly specific solute−solvent interactions, such as hydrogen bonds. In this case, the natural alternative is to construct molecular clusters formed by a few solvent molecules positioned at specific locations around the solute molecule.[44] On the other hand, it has been well-established that NMR chemical shifts can be accurately reproduced by the gauge-including atomic orbitals (GIAO) formalism combined with DFT methods,[45] even in molecular systems that include hydrogen-bonding interactions.[46,47]

In the present study, for the first time, the computation of ^{1}H and ^{13}C NMR spectroscopic parameters of a series of 1-alkyl-3-methylimidazolium salts was performed by the GIAO method at a B3LYP/6-31++G** level. The paper is organized in the following way. In the first section, the geometrical and energetic features of a series of molecular models of ionic liquid systems are analyzed. Different approaches to the ionic liquid environment have been used to estimate the molecular properties: (a) gas-phase model, including three cations: 1-methyl-, 1-butyl-, and 1-octyl-3-methylimidazolium ($Mmim^+$, $Bmim^+$, and $Omim^+$, respectively), three anions (PF_6^-, BF_4^-, and Br^-), and five ion pairs ($MmimPF_6$, $BmimPF_6$, $OmimPF_6$, BmimBr, and $BmimBF_4$); (b) PCM, to simulate nonspecific interactions in the solvated ionic liquid $MmimPF_6$ and its separated counterions $Mmim^+$ and PF_6^- with different solvents (water, dichloromethane, and benzene); and (c) molecular clusters formed by the ion-paired $MmimPF_6$ species (but also the separated cation $Mmim^+$ or anion PF_6^-) and a discrete number (one to three) of water molecules, to describe the specific solute−solvent interactions. The second section is devoted to the analysis of the computed NMR properties of the ionic liquids studied and introduces the influence of the environment and the interaction between counterions in the predicted NMR chemical shifts. In the concluding section, we use computational NMR results to analyze the available experimental data. As a result, theoretical and experimental NMR evidences are put into a more general perspective to assist in the understanding of the different factors that have a role in the NMR spectroscopic parameters of ionic liquids in condensed phases.

2. Computational Approach

Computational Methods. All of the molecular energies, geometries, frequencies, and dipole moments have been calculated using the B3LYP method[48,49] in conjunction with a 6-31++G** basis set. The presence of a minimum amount of energy was ensured by the lack of imaginary vibrational frequencies. All computations were performed with the aid of the Gaussian 03 program.[50]

Environment Simulation. The molecular structures of the ionic liquid species (ion pairs and independent cations and anions) were initially optimized in the gas phase, as a tentative molecular model in the absence of solvent. In order to describe nonspecific solvent effects, polar environments have been simulated by the latest version of the PCM.[51,52] Three solvents have been used: benzene ($\epsilon = 2.24$), dichloromethane ($\epsilon = 8.93$), and water ($\epsilon = 78.39$). Finally, molecular models of solvated ionic liquids including clusters with a discrete number (one to three) of water molecules have been calculated to simulate acidic and basic specific interactions with the solvent.

Energy of the Ion-Pair Formation (E_{IL}). Simplified models to describe the interaction between the cation and the anion in the ionic liquids have been applied using the different simulations of the ionic liquid environment. The gas-phase energy of the ion-pair formation has been estimated using the equilibrium described in eq 1 of Scheme 2. The calculated electronic energies of the solvated neutral ion-paired species and the freely dissolved counterions by the PCM approach have been applied in eq 2 of Scheme 2 to estimate the energy of ion-pair formation in a dielectric continuum environment. In addition, we have used the equilibria described in eqs 3 of Scheme 2 to estimate the energy of ion-pair formation when the ionic liquid is specifically solvated by acidic or basic solvent molecules.

SCHEME 3

$$\left.\begin{array}{lcl} (CA)_{\text{gas-phase}} & \leftrightarrow & (CA)_{\text{solvated}} \\ (C^+)_{\text{gas-phase}} & \leftrightarrow & (C^+)_{\text{solvated}} \\ (A^-)_{\text{gas-phase}} & \leftrightarrow & (A^-)_{\text{solvated}} \end{array}\right\} \quad \Delta E = E_{solvation} \qquad \text{Eqs. 4}$$

$$\left.\begin{array}{lcl} (CA)_{\text{gas-phase}} + (n\cdot H_2O)_{\text{gas-phase}} & \leftrightarrow & (CA)\cdot(H_2O)_n \\ (C^+)_{\text{gas-phase}} + n\cdot H_2O)_{\text{gas-phase}} & \leftrightarrow & (C^+)\cdot(H_2O)_n \\ (A^-)_{\text{gas-phase}} + (n\cdot H_2O)_{\text{gas-phase}} & \leftrightarrow & (A^-)\cdot(H_2O)_n \end{array}\right\} \quad \Delta E = E_{solvation} \qquad \text{Eqs. 5}$$

TABLE 1: Calculated Molecular Parameters (Electronic Energies, Bond Distances, Vibrational Frequencies, and Dipole Moments) of 1-Alkyl-3-methylimidazolium Ionic Liquids at a B3LYP/6-31++G Computational Level Using a Gas-Phase Model**

		E (au)	E_{IL}[a] (kcal/mol)	C2−H2 (Å)	N1−C2 (Å)	H2···F (Å)	X−F (Å)	ν(C2−H2)[b] (cm^{-1})	ν_a(X−F)[c] (cm^{-1})	μ (D)
					Gas-Phase Model					
ion pairs	$MmimPF_6$	−1246.087 914	−77.6	1.080	1.336	2.048	1.683	3282	845−849−862	15.0
	$BmimPF_6$	−1364.045 602	−76.7	1.080	1.337	2.133	1.677	3289	843−848−861	14.4
	$OmimPF_6$	−1521.315 467	−76.3	1.080	1.337	2.139	1.676	3290	842−848−861	14.3
	BmimBr	−2995.157 423	−92.2	1.075	1.338	2.781[d]		3336		9.2
	$BmimBF_4$	−847.905 778	−82.4	1.080	1.337	2.085	1.434	3277	974−1010−1173	12.6
ions	$Mmim^+$	−305.248 258		1.079	1.339			3298		0.8
	$Bmim^+$	−423.207 396		1.079	1.339			3298		5.7
	$Omim^+$	−580.477 801		1.079	1.338			3298		16.0
	PF_6^-	−940.7160 20					1.648		842 (×3)	0
	Br^-	−2571.803 183								0
	BF_4^-	−424.567 017					1.417		1052 (×3)	0

[a] Calculated by eq 1 of Scheme 2. [b] Stretching vibration of C2−H2 moiety of the cation. [c] Antisymmetric X−F stretching vibration of the anion, being X = P or B. [d] H2···Br distance.

Energy of Solvation ($E_{solvation}$). The net stabilization of energy due to interactions with the solvent for all of the neutral and charged ionic liquid structures has been computed by the following procedures: (a) continuum solvation model, where nonspecific interaction energies have been calculated using the PCM, following eqs 4 of Scheme 3, and (b) discrete solvation model, where the energy of stabilization of the gas-phase ionic liquid species when interacting with one to three water molecules has been calculated following eqs 5 of Scheme 3.

Free Energies (ΔG). Theoretical free energies have been predicted at the B3LYP/6-31++G** computational level including electronic energies, zero-point energies, enthalpy temperature corrections, and absolute entropies at selected temperatures and 1 atm and derived using the calculated vibrational frequencies and standard statistical thermodynamics relationships. Calculated free energies have been applied to the description of the chemical equilibria described in Scheme 2.

NMR Calculations. The isotropic ^1H and ^{13}C NMR nuclear shieldings were calculated at the B3LYP/6-31++G** level using the GIAO method.[53,54] The conversion to chemical shifts was done using the experimental−theoretical linear correlations between the experimental ^1H and ^{13}C NMR chemical shifts of pure $BmimPF_6$ and $BmimBF_4$ reported by Suarez et al.[14] and the corresponding calculated isotropic shieldings of the optimized ion pairs in the gas phase.

3. Results and Discussion

3.1. Preliminary Computational Analysis. *Gas-Phase Species.* To initiate the computational description of these compounds, we note that the ion-pair formation in the gas phase is accompanied by a significant stabilization of electronic energy ($E_{IL} < -75$ kcal/mol, see Table 1). Clear evidence of hydrogen-bonding effects on imidazolium salts with PF_6^- and BF_4^- anions are revealed by calculations: (a) The optimized geometry of the ion-paired species corresponds to a specific structure with the anion located above the imidazolium ring, close to the C2−H2 group, and slightly deviated toward the longer alkyl chain (see Figure 1 for $BmimPF_6$ and $BmimBF_4$). This is in good agreement with previous theoretical reports at different calculation levels.[40−42] (b) The frequencies of the stretching vibrations of the C2−H2 and X−F groups of the separated counterions are significantly different than those of the ion-paired structures; this is due to a well-known hydrogen bond effect (Table 1). (c) Even when calculations provide only slightly affected imidazolium structures by cation−anion interactions (see C2−H2 and N1−C2 in Table 1), the predicted X−F distances closer to the imidazolium ring noticeably increase from independent ions to ion pairs.

In order to understand the nature of the interaction between counterions, we have computed the electrostatic potential on an isosurface of electronic density around the $Bmim^+$ cation (Figure 2). Clearly, the electronic charge deficiency (blue color in Figure 2) observed around the C2−H2 group identifies it as the most acidic part of the imidazolium structure; therefore, the hydrogen-bond interaction with the nucleophilic F atoms of the anion would be favored. We observe, however, that calculations provide ionic liquid structures only slightly affected by the cation−anion interactions. The data in Figures 3 and 4 compare all of the calculated molecular distances and vibrations of the $BmimPF_6$ ion pair to those of the separated cation, $Bmim^+$, and anion, PF_6^-. Thus, we observe that only the distances and the vibrations of atomic groups involved in hydrogen bonds are significantly different in the ion pairs with respect to independent ions; that is, only C2−H2 and ($-CH_n-$) groups of the

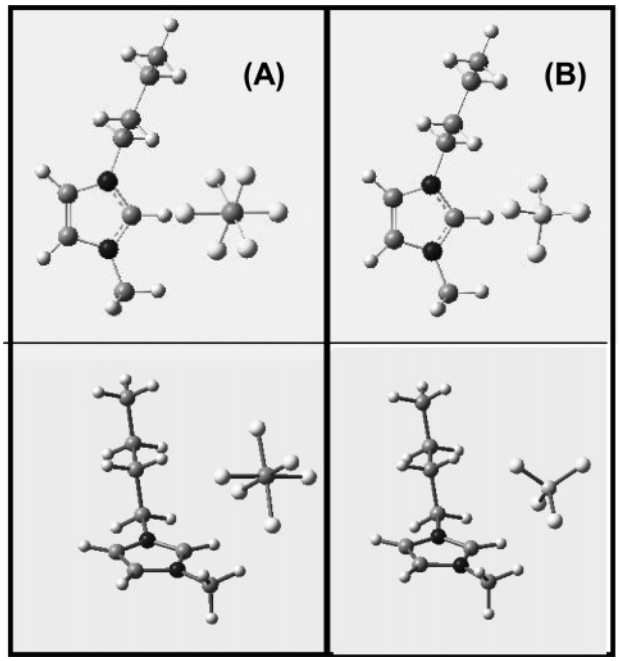

Figure 1. Molecular structure of $BmimPF_6$ (A) and $BmimBF_4$ (B) ion-paired species calculated at a B3LYP/6-31++G** computational level in the gas-phase environment.

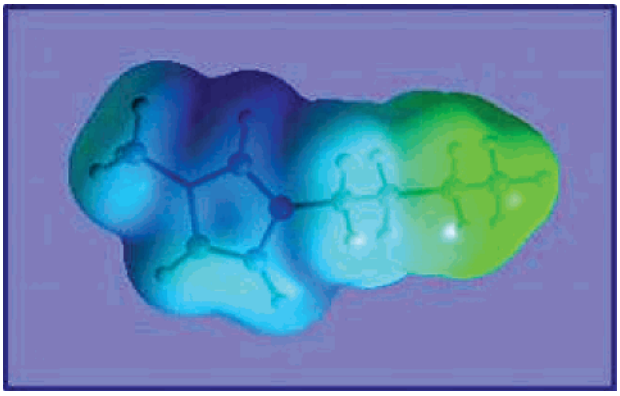

Figure 2. Representation of the electrostatic potential on an isosurface of electronic density (0.0004 au) for the $Bmim^+$ cation calculated at a B3LYP/6-31++G** computational level in the gas-phase environment.

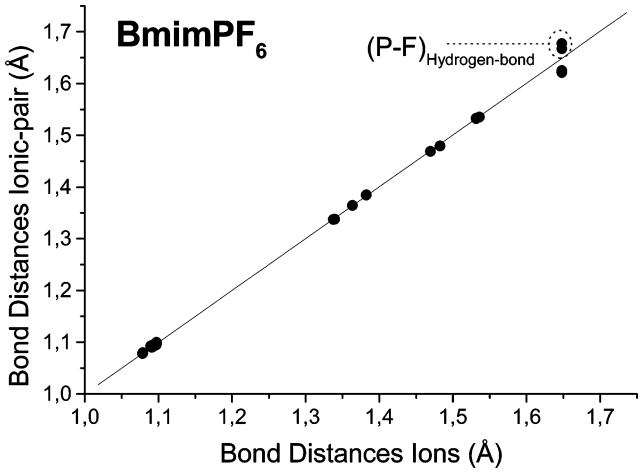

Figure 3. Calculated bond distances of the ion-paired structure versus the calculated bond distances of the independent cation and anion of $BmimPF_6$ obtained at a B3LYP/6-31++G** computational level in the gas-phase environment.

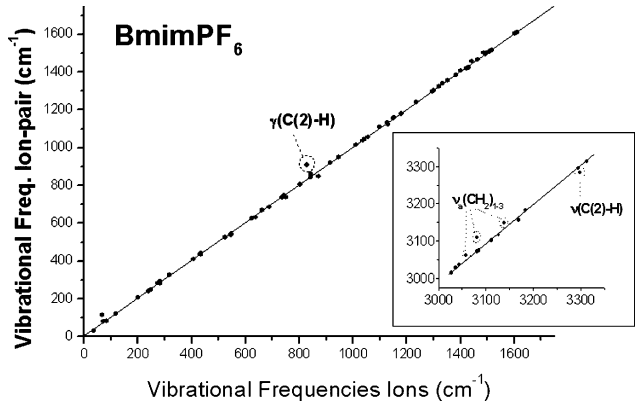

Figure 4. Calculated vibrational frequencies of the ion-paired structure versus the calculated vibrational frequencies of the independent cation and anion of $BmimPF_6$ obtained at a B3LYP/6-31++G** computational level in the gas-phase environment.

imidazolium ring specifically interact with the anion. These results suggest that the high energy of stabilization due to the ion-pair formation (E_{IL} in Table 1) should mainly be attributed to the electrostatic attraction between differently charged ions since hydrogen bonding is computationally predicted with a weak effect on the electronic structure of the ionic liquid species.

We may analyze the influence of the length of the alkyl group on the molecular properties of ionic liquids comparing the computational results for $MmimPF_6$, $BmimPF_6$, and $OmimPF_6$.

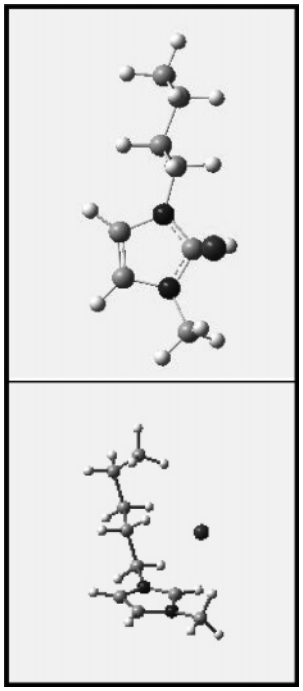

Figure 5. Molecular structure of the BmimBr ion-paired species calculated at a B3LYP/6-31++G** computational level in the gas-phase environment.

As it is shown in Table 1, calculated ion-pair formation energies (E_{IL}) and structural parameters (bond distances and vibrational frequencies) are almost unchanged by the length of the alkyl chain. Thus, only slightly less stabilized ionic-pair structures are found when the number of atoms increases in changing from a methyl substituent (E_{IL} = −77.6 kcal/mol) to an octyl substituent (E_{IL} = −76.3 kcal/mol). Coherently, the weak shortening of X−F bonds and the increasing of H2···F distances imply that there is a slightly weaker hydrogen bond in $OmimPF_6$ than in $MmimPF_6$. Since there was evidence of attractive interactions between the anion and the alkyl groups of the ring, the lower stability of an ion pair with prominent substituents should be related to the esteric effects.

On the other hand, the computational study of the $BmimPF_6$, $BmimBF_4$, and BmimBr structures allows us to analyze the effect of the anion on these common ionic liquids. First, we find that the energetic stabilization by ion-pair formation follows the order BmimBr > $BmimBF_4$ > $BmimPF_6$ (E_{IL} in Table 1). Moreover, current results reveal a different nature in the cation−anion interaction for the Br^- anion with respect to the PF_6^- or BF_4^- anions. Thus, whereas gas-phase calculations of $BmimPF_6$ and $BmimBF_4$ suggest the presence of hydrogen bonding between counterions, in the case of BmimBr, the anion is located more centered above the imidazolium plane, far from the acidic H2 atom (see Figure 5 and the Br···H2 distance in Table 1), and the alkyl groups rotate to interact with the anion. In fact, the effects of ion-pair formation on the bond distance and frequency of the C2−H2 group in BmimBr are just the opposite of those found in $BmimPF_6$ and $BmimBF_4$ compounds. On the other hand, current calculations provide evidence of a closer hydrogen-bond interaction between BF_4^- and $Bmim^+$ rather than with the PF_6^- anion (see C2−H2···F−X bond distances and frequencies collected in Table 1), which would explain the additional stabilization of 5.7 kcal/mol exhibited by $BmimBF_4$ compound.

Finally, calculations predict that all of the ionic liquids studied are strongly polar structures in the gas phase, with high dipole

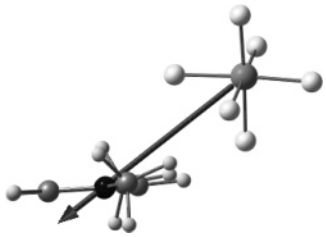

Figure 6. Representation of the molecular dipole orientation of the $MmimPF_6$ ion-paired species calculated at a B3LYP/6-31++G** computational level in the gas-phase environment.

moment vectors (up to 12 D), orientated as it is shown in Figure 6. Moreover, computational results reveal a slightly lower polarity in the ionic-pair structure by increasing the size of the alkyl chain (from $\mu_{MmimPF_6} = 15.0$ D to $\mu_{OmimPF_6} = 14.3$ D). In addition, we find that the dipole moment of the ion-paired species is strongly affected by the type of anion considered (see Table 1). Thus, among the three anions studied, an increase in polarity is predicted when the anion is located farther from the imidazolium ring ($\mu_{BmimPF_6} = 14.4$ D > $\mu_{BmimBF_4} = 12.6$ D > $\mu_{BmimBr} = 9.2$ D).

Solvated Species. We will consider the net energy of solvation (eqs 4 in Scheme 3; $E_{solvation}$ in Table 2) of $MmimPF_6$ structures related to the nonspecific interactions with the solvent, using the PCM. First, we find significant stabilization by solvent effects in all ionic liquid species studied. However, notably more effective nonspecific interactions occur with the ionic species $Mmim^+$ and PF_6^- than with the ion pair $MmimPF_6$, which is becoming more evident in more polar solvents (Table 2). In order to analyze the consequences of these results, we have computed the energy of the ion-pair formation in $MmimPF_6$ using the PCM to simulate the dielectric continuum environments [eq 2 in Scheme 2; $(E_{IL})_{solvation}$ in Table 2]. Significantly, calculations show that the ion-pair formation energy in $MmimPF_6$ diminishes drastically with the polarity of the solvent: from E_{IL}(gas-phase medium) = −77.6 kcal/mol (Table 1) to E_{IL}(water medium) = −0.2 kcal/mol (Table 2). In fact, we find that the ion-pair $MmimPF_6$ species are scarcely energetically favored in water. Moreover, the analysis of the optimized geometries reveal an anion located farther from the imidazolium ring in the solvated $MmimPF_6$ ion pair when the dielectric constant of the solvent increases (see the calculated C2−H2, H2··F, and P−F bond distances in Table 2). Therefore, the PCM for $MmimPF_6$ indicates the weakening of the hydrogen bond between counterions determined by the polarity of the environment. Additionally, we find an increase in the dipole moment of the ion-pair $MmimPF_6$ structure when it goes from the gas phase (μ = 15.0 D) to water (μ_{MmimPF_6} = 21.5 D) polarity, which is probably associated with the rise of the cation−anion distance.

Furthermore, we have used a discrete solvation model of the ionic liquid to simulate the specific acidic and basic interactions with the solvent on the basis of molecular clusters formed by ionic liquid $MmimPF_6$ species and a variable number of water molecules (n = 1−3). To initiate the analysis, we computed the energy of solvation of the $MmimPF_6$ species by one to three water molecules (eqs 5 in Scheme 3; $E_{solvation}$ in Table 2). We find that the $MmimPF_6$ ion pair is stabilized 11.2 kcal/mol by the interactions with one water molecule. In addition, the $E_{solvation}$ values when $MmimPF_6{\cdot}(H_2O)_n$ clusters include two (n = 2) or three (n = 3) water molecules are respectively −21.2 and −26.1 kcal/mol. In summary, calculations predict that each addition of one molecule of water stabilizes the ion-pair $MmimPF_6$ structure by approximately 10 kcal/mol. As it is shown in Figure 7, the optimized geometries of predicted clusters contain the nucleophilic oxygen atom of water orientated toward the C2−H2 and alkyl groups of the imidazolium ring, whereas the acidic hydrogen atoms of water are attracted by the anion. In fact, the

TABLE 2: Calculated Molecular Parameters (Electronic Energies, Bond Distances, Vibrational Frequencies, and Dipole Moments) of the $MmimPF_6$ Ionic Liquid at a B3LYP/6-31++G Computational Level Using the PCM and Discrete (Clusters) Solvation Model**

		E (au)	$E_{solvation}$ (kcal/mol)	$(E_{IL})_{solvated}$[c] (kcal/mol)	C2−H2 (Å)	H2···F (Å)	P−F (Å)	ν(C2−H2)[d] (cm^{-1})	ν_a(P−F)[e]/$\nu_{s,a}$(O−H)[f] (cm^{-1})	μ (D)
				PCM						
benzene	$MmimPF_6$	−1246.106 850	−11.9[a]	−31.4	1.079	2.152	1.669	3298	822−824−837	17.7
	$Mmim^+$	−305.292 023	−27.5[a]		1.083			3245		0.8
	PF_6^-	−940.764 742	−30.6[a]				1.647		819 (×3)	0
DCM	$MmimPF_6$	−1246.124 893	−23.2[a]	−6.9	1.079	2.253	1.658	3300	800−803−812	21.1
	$Mmim^+$	−305.319 651	−44.8[a]		1.086			3183		0.9
	PF_6^-	−940.794 277	−49.1[a]				1.646		796 (×3)	0
water	$MmimPF_6$	−1246.132 098	−27.7[a]	−0.2	1.080	2.389	1.652	3285	788−791 − 800	21.5
	$Mmim^+$	−305.328 508	−50.3[a]		1.088			3154		0.9
	PF_6^-	−940.803 303	−54. [a]				1.646		784 (×3)	0
				Discrete Solvation Model (Clusters)						
$MmimPF_6{\cdot}H_2O$		−1322.539 968	−11.2[b]	−78.3	−78.3	1.339	1.640	3258	825−863−864	13.0
$MmimPF_6\ (H_2O)_2$		−1398.989 942	−21.2[b]	−77.0	−77.0	1.342	1.637	3245	852−858−860	14.0
$MmimPF_6\ (H_2O)_3$		−1475.431 946	−26.1[b]	−70.3	−70.3	4.924	1.640	3191	854−857−871	17.6
$Mmim^+{\cdot}H_2O$		−381.700 302	−11.2[b]		1.085			3219	3795−3899	1.0
$Mmim^+\ (H_2O)_2$		−458.152 510	−22.5[b]		1.088			3171	3562−3871	0.8
$Mmim^+\ (H_2O)_3$		−534.601 383	−31.8[b]		1.092			3114	3618−3690	0.7
$PF_6^-{\cdot}H_2O$		−1017.166 920	−10.5[b]				1.662		835−836−859/ 3788−3847	1.1
$PF_6^-\ (H_2O)_2$		−1093.619 456	−22.1[b]				1.664		842−843−851/ 3768−3826	2.2
$PF_6^-\ (H_2O)_3$		−1170.066 901	−30.5[b]				1.674		829−842−864/ 3798−3869	2.4

[a] Calculated by eqs 4 of Scheme 3. [b] Calculated by eqs 5 of Scheme 3. [c] Calculated by eqs 3 of Scheme 2. [d] Stretching vibration of C2−H2 of the cation. [e] Antisymmetric P−F stretching vibration of the anion. [f] Symmetric and antisymmetric O−H stretching vibration of water molecule in cluster.

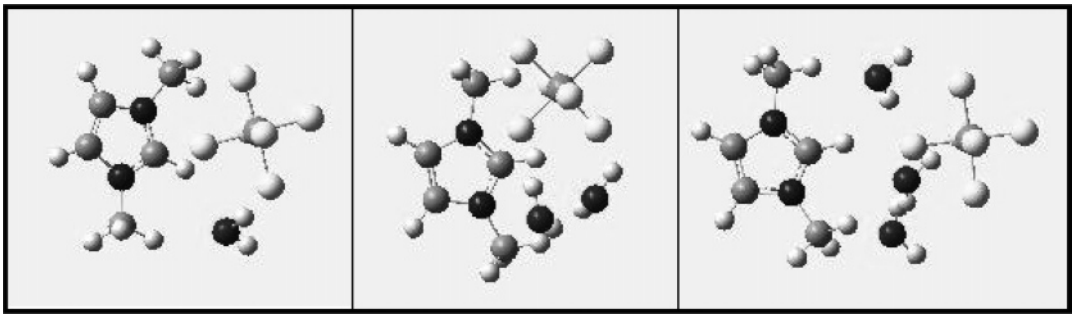

Figure 7. Molecular structure of the clusters formed by the $MmimPF_6$ ion pair and a number (one to three) of water molecules optimized at a B3LYP/6-31++G** computational level.

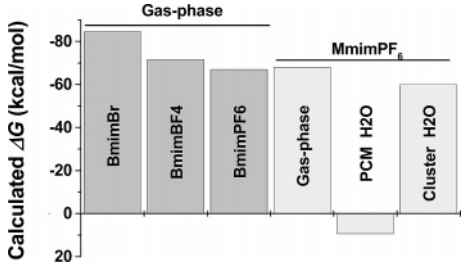

Figure 8. Theoretically calculated free energies of the ion-pair formation (following eqs 1−3 of Scheme 2) of 1-alkyl-3-methylimidazolium salts obtained by different computational approaches of the environments (gas phase, continuum, and discrete solvation models of water solvent) at 298 K and 1 atm using a B3LYP/6-31++G** computational level.

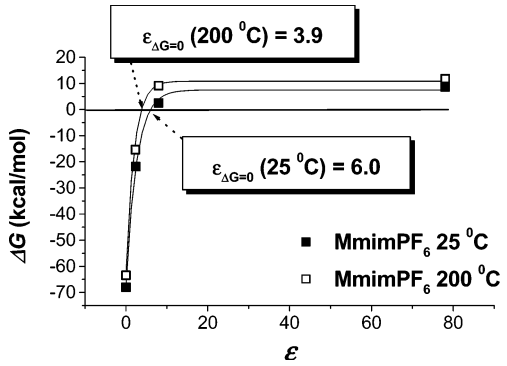

Figure 9. Predicted solvent polarity dependence of the free energies of the $MmimPF_6$ ion-pair formation (following eq 2 of Scheme 2) calculated by using the PCM at a B3LYP/6-31++G** computational level.

calculated H2···F distance (4.9 Å) of the cluster $MmimPF_6 \cdot (H_2O)_3$ clearly indicates the absence of hydrogen bonding between the acidic C2−H2 group of the imidazolium ring and the anion (Table *2*). Otherwise, the specific interactions detected between counterions are completely replaced by new and more effective hydrogen bonds with the donor and acceptor groups of water (see the characteristic bond distances and vibrational frequencies of the $MmimPF_6 \cdot (H_2O)_3$ cluster in Table 2). In this sense, it is notorious that independent anionic ($Mmim^+$) and cationic (PF_6^-) species present a stabilization of energy similar to that for ion pairs (eqs 4 in Scheme 3; E_{IL} in Table 2) because of the interaction with the water molecules. In fact, the calculations of the ion-pair formation energies using the discrete model of solvation [eqs 3 in Scheme 2; $(E_{IL})_{solvation}$ in Table 2] show that the formation of $MmimPF_6 \cdot (H_2O)_n$ aggregates is accompanied by a stabilization higher than 70 kcal/mol, with independency of the water molecules added. In summary, computational results predict that the $MmimPF_6$ ionic liquid in water solution formed by solvent-separated ion pairs instead of by fully associated ion pairs surrounded by water molecules.

To complete this preliminary computational analysis, we have also calculated the free energies of the simplified equilibria ($A^+ + C^- \leftrightarrow AC$) described in Scheme 2 taking into account the gas phase (eq 1), continuum (eq 2), and discrete (eqs 3) molecular environments. Results in Figure 8 show that the formation of an ion-paired species is thermodynamically favored in the gas phase for all of the ionic liquids considered (equilibrium of eq 1). In contrast, the PCM for water predicts that the equilibrium is mainly displaced toward the freely dissolved ions by the polarity of the solvent. As a matter of fact, we show in Figure 9 the calculated free energies of the ion-pair $MmimPF_6$ formation (equilibrium of eq 2) using increasing dielectric constants of the solvent [from $\epsilon = 0$ (gas phase) to $\epsilon = 78$ (water)]. One can observe that the formation of ion-paired structures is predicted only spontaneously in low-dielectric solutions. In other words, the current computational study predicts that the chemical equilibrium for the $MmimPF_6$ compound lies in favor of independent solvated ions in a medium as low in polarity as dichloromethane. Additionally, we have calculated the free energy of the ion-pair $MmimPF_6$ formation using the discrete solvation model (equilibria of eqs 3), on the basis of clusters formed by ionic liquid species and water molecules. Figure 8 shows the result for the case of the $MmimPF_6 \cdot (H_2O)_3$ aggregate. Thus, the discrete solvation model predicts the spontaneous formation of clusters consisting of a hydrogen-bonded network, with water molecules as an acceptor toward the cation and as a donor toward the anion, replacing progressively the C−H···F interactions between counterions.

3.2. NMR Calculations. *Gas-Phase Species.* In Figure 10, the ^1H and ^{13}C NMR chemical shifts of pure $BmimPF_6$ and $BmimBF_4$ ionic liquids reported by Suarez et al.[14] are compared to the corresponding isotropic shieldings of the gas-phase ion pairs calculated in this work using the GIAO−B3LYP/6-31++G** method. The good agreement between experimental and theoretical NMR data allows us to confirm the assignment of NMR peaks performed by these authors and others before us.[11−13] In addition, we have used the linear relationships for these data to convert the isotropic chemical shielding in chemical shifts in order to simulate the ^1H and ^{13}C NMR spectra of the ionic liquids studied. As a result, Tables 3 and 4 collect respectively the ^1H and ^{13}C NMR chemical shifts for 1-alkyl-3-methylimidazolium ionic liquids calculated in this work, including isolated and solvated ion pairs but also separated counterions.

Since the ^1H and ^{13}C NMR spectra of the gas-phase ion-paired structures adequately reproduce the experimental ones of pure $BmimPF_6$ and $BmimBF_4$ ionic liquids, it is concluded that H2 exhibits a larger downfield shift than H4 and H5, which present very close ^1H NMR chemical shifts, in good agreement with Seddon et al.'s findings.[11] As it was shown before, the

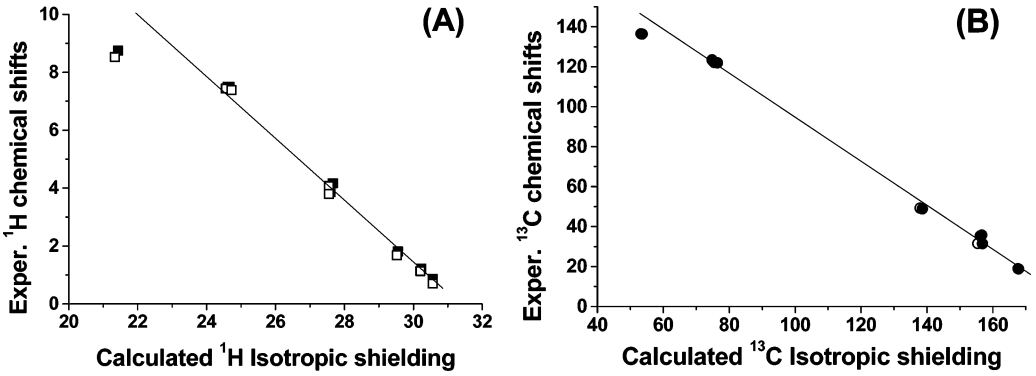

Figure 10. Comparison of calculated ^{1}H (A) and ^{13}C (B) NMR isotropic shielding by the GIAO−B3LYP/6-31++G** method and experimentally obtained ^{1}H and ^{13}C NMR chemical shifts of the $BmimPF_6$ (solid) and $BmimBF_4$ (open) ionic liquids reported by Suarez et al.[14]

hydrogen atom at position 2 presents a more acidic character; however, the difference between H2 and H4/H5 chemical shifts (Table 3) is visibly increased from the ion pairs to the corresponding separated cations, which must be attributed to the location of the nucleophilic F atoms of the anion that are very close to the donor group C2−H2 of the imidazolium ring. Therefore, current calculated ^{1}H NMR parameters indicate not only the presence of hydrogen bonding between the counterions of 1-alkyl-3-methylimidazolium ionic liquids, as identified from NMR experiments,[11,12,14,16] but also the presence of tight ion pairs in the pure state of these compounds, which coincides with Mele et al.'s conclusions in their NOEs and ROEs NMR studies.[19] It should be noted, however, that the downfield effect on the H2 chemical shift is overestimated in the gas-phase model with respect to the experimental liquid phase.

On the other hand, the comparison between the calculated ^{1}H and the ^{13}C NMR parameters of ionic liquid species (Tables 3 and 4) shows similar effects on the chemical shifts of the interaction between counterions.

In order to analyze the effect of the alkyl group on magnetic properties, we have computed the ^{1}H and ^{13}C NMR spectra of the gas-phase optimized structures of $MmimPF_6$, $BmimPF_6$, and $OmimPF_6$ compounds. Computational results collected in Tables 3 and 4 showed that the length of the alkyl groups at the N1 position does not significantly influence the chemical shifts of the hydrogen and carbon atoms of the imidazolium ring, which is consistent with previous experimental observations.[12,15,20,22] On the other hand, calculations show a strong anion dependence of the ^{1}H and ^{13}C NMR chemical shifts for $BmimPF_6$, $BmimBF_4$, and BmimBr compounds (Tables 3 and 4), which has been extensively reported in experimental NMR works.[11,12,14,17] We find that ^{1}H chemical shifts of the 1-butyl-imidazolium ring and alkyl chains generally increase with the increase of anion basicity ($Br^- < PF_6^- < BF_4^-$), but this effect is more significant in the case of C2−H2, which is directly involved in the hydrogen-bonding interaction between counterions. Moreover, calculated ^{1}H NMR data in the gas-phase model are consistent with a more effective interaction between counterions in $BmimBF_4$ rather than those in $BmimPF_6$, in coherence with the results obtained in the previous section and the experimental reports of Headley et al.[18,22] but opposite to ^{1}H NMR data reported by Suarez et al.[14] It should be noted, however, that the calculated ^{13}C NMR data show slightly lower downfield shifts in $BmimBF_4$ than in $BmimPF_6$, which in this case reproduce ^{13}C NMR data reported by Suarez et al.[14]

Solvated Species. The next step of this study will be to compute the NMR parameters of the solvated ionic liquid $MmimPF_6$ using both continuum and discrete computational

TABLE 3: Calculated ^{1}H NMR Chemical Shifts of 1-Alkyl-3-methylimidazolium Ionic Liquids by the GIAO−B3LYP/6-31++G Method Using Different Simulations of the Ionic Liquid Environment (Gas Phase, Discrete Solvation Model, and PCM of Water)**

		H2	H4	H5	H_{CH_2},alkyl	H_{CH_3},alkyl	H_{CH_3}
			Gas-Phase Model				
ion pairs	$MmimPF_6$	10.16	7.08	7.08		4.25	4.25
	$BmimPF_6$	10.14	7.06	7.12	4.21	1.47	4.25
	$OmimPF_6$	10.11	7.05	7.12	4.21	1.30	4.26
	BmimBr	9.67	6.66	6.76	3.90	1.46	4.05
	$BmimBF_4$	10.23	7.08	7.16	4.33	1.42	4.33
ions	$Mmim^+$	7.74	7.62	7.62		4.22	4.22
	$Bmim^+$	7.74	7.55	7.57	4.16	1.60	4.27
	$Omim^+$	7.67	7.57	7.58	4.16	1.42	4.23
			PCM				
benzene	$MmimPF_6$	9.49	7.44	7.44		4.20	4.20
	$Mmim^+$	8.02	7.77	7.77		4.17	4.17
H_2O	$MmimPF_6$	8.65	7.94	7.94		4.17	4.17
	$Mmim^+$	8.47	7.99	7.99		4.16	4.16
			Discrete Solvatioin Model (Clusters)				
$MmimPF_6 \cdot H_2O$		10.21	7.09	7.09		4.32	4.44
$MmimPF_6 (H_2O)_2$		10.46	7.10	7.10		4.42	4.48
$MmimPF_6 (H_2O)_3$		10.94	7.11	7.11		4.51	4.80
$Mmim^+ \cdot H_2O$		9.78	7.57	7.57		4.18	4.37
$Mmim^+ (H_2O)_2$		10.57	7.52	7.52		4.16	4.47
$Mmim^+ (H_2O)_3$		11.39	7.46	7.46		4.14	4.47

TABLE 4: Calculated ^{13}C NMR Chemical Shifts of 1-alkyl-3-methylimidazolium Ionic Liquids by GIAO−B3LYP/6-31++G Method Using Different Simulation of the Ionic Liquid Environment (Gas Phase, Discrete Solvation Model, and PCM of Water)**

		C2	C4	C5	$C_{CH2,alkyl}$	$C_{CH3,alkyl}$	C_{CH3}
			Gas-Phase Model				
neutrals	$MmimPF_6$	136.8	114.9	115.2		37.5	37.5
	$BmimPF_6$	135.4	115.0	114.2	55.0	18.0	37.4
	$OmimPF_6$	135.7	115.1	113.8	54.4	19.2	37.2
	BmimBr	126.2	114.6	109.9	54.5	18.0	39.7
	$BmimBF_4$	135.1	114.9	113.4	54.3	18.2	37.0
ions	$Mmim^+$	126.5	119.3	119.3		38.6	38.6
	$Bmim^+$	125.6	118.4	118.8	56.0	17.8	38.3
	$Omim^+$	125.3	118.2	118.4	55.9	18.6	38.5
			PCM				
benzene	$MmimPF_6$	133.7	116.3	116.3		37.3	37.3
	$Mmim^+$	127.3	119.2	119.2		38.3	38.3
H_2O	$MmimPF_6$	130.1	118.4	118.4		37.4	37.4
	$Mmim^+$	128.9	119.0	119.0		37.8	37.8
			Discrete Solvatioin Model (Clusters)				
$MmimPF_6 \cdot H_2O$		135.5	115.9	113.9		38.0	39.9
$MmimPF_6 \cdot (H_2O)_2$		134.9	115.4	115.3		38.5	39.5
$MmimPF_6 \cdot (H_2O)_3$		134.7	116.5	114.9		38.0	39.9
$Mmim \cdot H_2O$		130.5	118.6	118.2		37.9	38.1
$Mmim^+ \cdot (H_2O)_2$		132.2	117.8	117.8		37.6	37.9
$Mmim^+ \cdot (H_2O)_3$		133.5	117.3	117.3		37.6	37.8

approaches to simulate the water environment. The two principal aspects analyzed in this section will be (a) the influence of the solvent media on the computed ^1H and ^{13}C NMR spectra of the 1-alkyl-3-methylimidazolium salts considered and (b) the characterization of the NMR signals corresponding to the different ionic liquid species in solution.

First, we will consider the NMR results of the ion-paired $MmimPF_6$ species calculated by the PCM of solvation (Tables 3 and 4). As Figure 11A clearly shows, the predicted ^1H chemical shift of H2 is strongly affected by the polarity of the solvent, moving to lower values. In contrast, the ^1H chemical shifts of H4 and H5 show substantial downfield shift when the dielectric constant of the solvent increases. On the other hand, we find that ^{13}C chemical shifts of the $MmimPF_6$ ion pair move in the same direction as the ^1H chemical shift because of the nonspecific interactions with the solvent but to a minor extent (Figure 11B). We consider the predicted changes of ^1H and ^{13}C NMR data shown in Figure 11 to be a direct consequence of the hydrogen bond weakening between counterions because of the interaction with the solvent field, as was shown in the above section. Second, we have computed the NMR properties of $MmimPF_6$ ion pair when it is specifically solvated by water molecules, that is, applying the discrete model of solvation. More importantly, we observe in Figure 12 that the ^1H chemical shift of the H2 atom exhibits a higher downfield shift when the specific interactions with the water molecules increase. Different results are found for the ^{13}C chemical shift of C2, which diminishes with the number of water molecules. On the basis of the comparison with the NMR results of separated ions, we concluded that the higher shielding of C2 of the $MmimPF_6$ ion pair with water should be assigned to a stronger ionic character of the imidazolium ring in the specifically solvated ionic liquid of water. In summary, current computational results reveal a clearly different behavior of the magnetic properties of ionic liquids when specific and nonspecific solute−solvent interactions are included in the calculation.

Current NMR calculations may be applied as a valuable tool to distinguish the presence of ionic liquid species that could coexist in solution. In order to easily visualize the predicted NMR signals, we compare in Figure 13 the ^1H NMR spectra

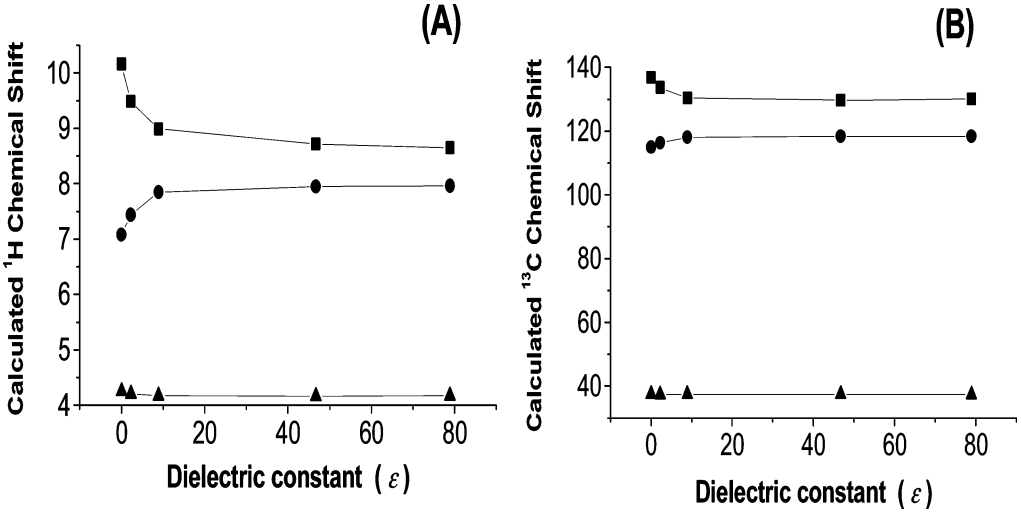

Figure 11. Predicted solvent polarity dependence of the ^1H (A) and ^{13}C (B) NMR chemical shifts of the $MmimPF_6$ ion pair calculated by using the PCM in conjunction with the GIAO−B3LYP/6-31++G** method.

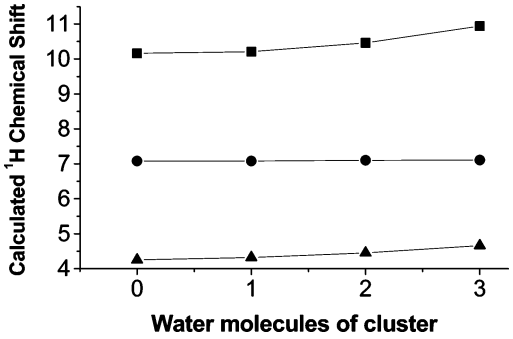

Figure 12. Predicted acidic and basic solvent dependence of the ^{1}H NMR chemical shifts of the $MmimPF_6$ ion pair calculated using a discrete solvation model based on clusters, formed by the $MmimPF_6$ structure and by a number of water molecules, optimized at a B3LYP/6-31++G** level.

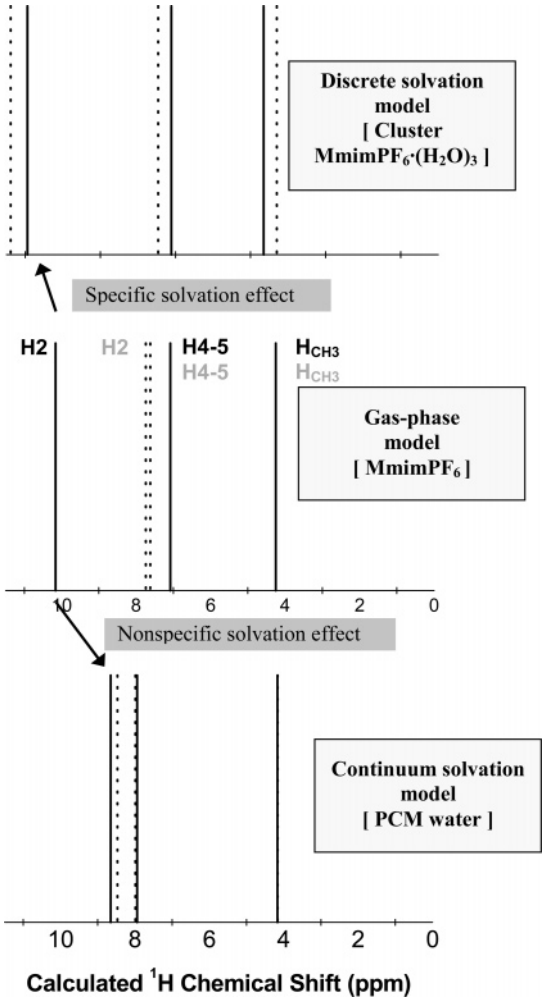

Figure 13. Theoretically calculated ^{1}H NMR spectra of the ion pair (solid lines) and separated cation (dotted lines) of $MmimPF_6$ by the GIAO−B3LYP/6-31++G** method using different simulations of the ionic liquid environment (gas phase, discrete solvation model, and PCM of water).

obtained for the separated cation and the ion-pair structure of $MmimPF_6$ using the different ionic liquid environments simulated in this work. First, the ^{1}H NMR signal of the H2 atom in the ion-paired structure in the gas phase is clearly separated from the one corresponding to the independent cation. Second, both the discrete model and the PCM predict ^{1}H NMR spectra of $MmimPF_6$ not easily distinguishable to that of the solvated cation. On the other hand, Figure 13 shows the different dependence of the ^{1}H chemical shift of $MmimPF_6$ on the nature

TABLE 5: Thermodynamic Data Related to the Equilibrium $C^+ + A^- \leftrightarrow CA$ Experimentally Obtained for EmimTfN[21] and Theoretically Predicted for MmimPF6 by PCM-B3LYP/6-31++G Calculations**

		ΔG (kcal/mol)		ΔH (kcal/mol)	
$C^+ + A^- \leftrightarrow CA$		$\epsilon = 4.30$	$\epsilon = 5.24$	$\epsilon = 4.30$	$\epsilon = 5.24$
298 K	EmimTfN	−4.4	−1.0	−11.6	−1.7
	$MmimPF_6$	−7.2	−2.7	−17.0	−12.5

of interactions with the solvent media. Thus, the discrete solvation model (based on $MmimPF_6{\cdot}(H_2O)_n$ clusters) reveals that hydrogen-bond interactions between the imidazolium ring and the water molecules imply a significant downfield shift in the H2 signal for both the cationic and the ion-paired species. In contrast, the PCM predicts that high-polar environment effects strongly move the chemical shift of H2 in the ion-paired $MmimPF_6$ species to lower values.

Finally, current computational results suggest a limited usefulness of ^{13}C NMR spectroscopy to analyze the different solvent effects on ionic liquid species possibly present in solution (Table 4).

3.3. Analysis and Discussion on Experimental NMR Data. In what follows, we will summarize the reported theoretical results to interpret the experimental NMR evidence mentioned in References and Notes, with special emphasis on the next main questions:

(a) NMR Evidence of Chemical Equilibrium between Ionic Liquid Species. Tubbs and Hoffman[21] found two sets of resonance features in the ^{1}H NMR spectrum of EmimTfN when the dielectric constant solvent media were gradually changed from CCl_4 ($\epsilon = 2.2$) to acetone ($\epsilon = 20.7$). The assignment of these ^{1}H NMR resonance sets to both freely dissolved ions and freely dissolved ion-paired aggregates as equilibrium species in solution is fully supported by our calculations. Thus, the authors identify the ^{1}H peak at 8.83 ppm as the H2 chemical shift of the separated cation, whereas the ^{1}H peak appearing at 8.57 ppm is assigned to the H2 signal of the ion-paired species. In good concordance, calculations on the $MmimPF_6$ compound in the presence of basic solvent molecules (water and acetone) predict the H2 chemical shift in the $MmimPF_6{\cdot}(H_2O)_n$ clusters at higher values rather than in the PCM solvated ion-paired species (see Figure 13). Moreover, Tubbs and Hoffman found that the equilibrium $C^+ + A^- \leftrightarrow CA$ is quantitatively displaced to dissolved ions at solvent dielectric constants higher than $\epsilon = 5.4$ at 298 K for EmimTfN. Meanwhile, current calculations predict this change at $\epsilon = 6.0$ for the case of the $MmimPF_6$ ionic liquid. In fact, we find an amazingly good agreement between the thermodynamic data experimentally obtained for the EmimTfN compound and the theoretically predicted data for $MmimPF_6$, as it can be seen in Table 5.

On the other hand, the phase change detected in $BmimBF_4$ (279 K) and $BmimPF_6$ (353 K) by Suarez et al.[14] and also in the ionic liquid $EmimBF_4$ (333 K) by Wang et al.,[17] which were ascribed to the decomposition of the ion-paired structures, may be explained by calculations if one considers the static dielectric constants of these imidazolium-based ionic liquids determined by Weingärtner et al.[55] at 298 K ($\epsilon_{BmimBF_4} = 11.7$, $\epsilon_{BmimPF_6} = 11.4$, and $\epsilon_{EmimBF_4} = 12.8$). Thus, we show in Figure 14 the predicted free energies of $BmimBF_4$ and $BmimPF_6$ (eq 2 in Scheme 2) estimated using the calculated gas-phase ΔG_{IL} values at 279 and 353 K, respectively, in conjunction with the first-order exponential regression obtained in Figure 9 for $MmimPF_6$. We observe that the predicted equilibrium constants for $BmimBF_4$ at 279 K and $BmimPF_6$ at 353 K are favorable to the individual ions at $\epsilon > 12$. These results seem to agree fairly

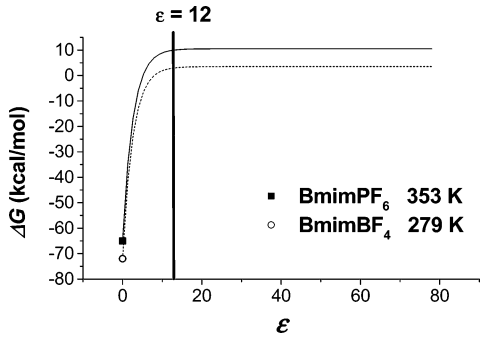

Figure 14. Predicted solvent polarity dependence of the free energies of ion-pair formation (following eq 2 of Scheme 2) of $BmimPF_6$ and $BmimBF_4$ calculated using the gas-phase free energy value at 353 K and 279 K, respectively, at a B3LYP/6-31++G** level, in conjunction with the first-order exponential regression obtained in Figure 9 for the $MmimPF_6$ case [$\Delta G = 8 - 40e^{(\epsilon/5)E80}$ (kcal/mol)].

well with the hypothesis of a dual behavior of these neat ionic liquids: quasi-molecular ion-paired species below the temperature of the phase change and cations and anions in an extended hydrogen-bonded network at higher temperatures.

Finally, Lin et al.,[20] on the basis of the ^1H and ^{13}C NMR measurements of methylimidazolium salts, concluded that ionic liquid compounds with BF_4^- and PF_6^- anions are presumed present in the ionic state when they are dissolved in high-polar solvents. The hypothesis of these authors seems to be nicely confirmed by our calculations, which predict the main presence of separated ions of $MmimPF_6$ in environments characterized by dielectric constants higher than $\epsilon = 6$ (see Figure 9). In addition, Headley et al.,[22] using ^1H NMR spectroscopy as well to study different imidazolium salts with BF_4^- and PF_6^- anions, concluded that strong hydrogen-bond interactions between the acidic groups of the cation and the solvent molecules result in a reduced interaction of the imidazolium ring with the anion. In this sense, Mele et al.[19] also using NMR experiments on the pure ionic liquid $BmimBF_4$ concluded that the presence of a small number of water molecules changes the structure of an ionic liquid through the participation of water in hydrogen bonding with the ions, replacing the C−H···F interactions between counterions. In agreement with cited experimental works, the molecular clusters optimized in our study show that, effectively, water molecules form hydrogen bonds with both cationic and anionic species of the ionic liquid. Indeed, calculations predict that only a few water molecules are necessary to completely replace the hydrogen-bond interactions between counterions (see Figure 7 and C2−H2···F distances in Table 2). In fact, strongly stabilized aggregates of water and charged species of the ionic liquid are predicted by the current computational approach [$(E_{IL})_{solvated}$ in Table 2 as described in eqs 3 of Scheme 2].

Concerning the effect of the ionic liquid concentration reported by Grätzel et al.,[12] we think that the increase of the ionic liquid concentration shifts the equilibrium toward the ion-pairing species in solution. As a result, the H2 chemical shift globally diminishes with the concentration. The initially higher H2 downfield found in the case of stronger basic anions at very low concentrations may be related to the expected more effective solvation of their ionic species.

(b) Solvent Effects on NMR Chemical Shifts of Ionic Liquids. In general, all of the spectroscopic NMR studies found in References and Notes on 1-alkyl-3-methylimidazolium ionic liquids used high-polar and basic solvents (dimethylsulfoxide, pyridine, nitromethane, water, etc.).[18,20,22] In such conditions, ionic liquids must be dissolved mainly as freely solvated ions. For the case of 1-alkyl-3-methylimidazolium salts with BF_4^- and PF_6^- anions, it is generally observed that the H2 chemical shift increases with the polarity of the solvent. In agreement, the developed model of solvation based on $MmimPF_6{\cdot}(H_2O)_n$ and $Mmim^+{\cdot}(H_2O)_n$ clusters indicates an increase of the H2 chemical shift value in the solvated cation (see Figure 13), which could be explained in terms of hydrogen bonding with the molecules of basic solvents. Furthermore, the PCM also provides a downfield H2 chemical shift at a higher solvent polarity. However, this H2 signal appears in a different position in the ^1H NMR spectra of $MmimPF_6$ if specifically or nonspecifically solvated ionic liquid species are considered.

For confirming the nature of the solvent effect on the ^1H chemical shifts of H2 atoms, we have performed a multilinear regression analysis of the experimental NMR data of imidazolium hexafluorophosphate salts involving the parameters of the empirical solvent scales of polarity-polarizability (SPP), basicity (SB), and acidity (SA) developed by Catalán et al.[56−58] Significantly, we obtain reasonable correlations between experimental H2 chemical shifts and solvent scale parameters (Table 6). Moreover, the signs of the coefficients for these SPP, SB, and SA parameters reveal a downfield change of the H2 chemical shift by the effect of the solvent basicity (SB), whereas the polarity of the medium moves this ^1H peak to lower chemical shifts (SPP). Then, the specific interactions with the solvent molecules change this H2 chemical shift in the opposite direction of the nonspecific polarization effects of the solvent cage. Noticeably, these empirical results are in full concordance with the predicted ^1H NMR data of $MmimPF_6$ by quantum-chemical calculations using the different models of solvation proposed (cluster and PCM). Therefore, we conclude that the NMR parameters of ionic liquids in solution are controlled by a complex sum of phenomena, including basic and acidic interactions together with dipole and polarizability interactions between solute and solvent.

Current results help us to understand the different NMR data behavior given in References and Notes for 1-alkyl-3-methylimidazolium halide ionic liquids. Thus, Lin et al.[20] reported BmimBr and EmimBr as compounds with an especially large ^1H NMR chemical shift dependence on the solvent nature, in concordance with previous spectroscopic studies published.[59] Lin et al.[20] concluded that the bromide ion generates less ionizable ionic liquids than BF_4^- and PF_6^- anions. Calculated free energies of the $C^+ + A^- \leftrightarrow CA$ equilibrium in vacuum for 1-butyl-3-methylimidazolium compounds (Figure 9) aid that conclusion. In fact, the experimental H2 chemical shifts of EmimBr by solvent effect are consistent with those predicted by the ion-pair structure in solution (PCM of Figure 13), because

TABLE 6: Correlation Equations Showing the Relationship between the Experimental ^1H NMR Chemical Shift for the H2 Atom of Imidazolium Salts and the Solvent Parameters of SPP, SB, and SA Developed by Catalán et al.[56−58]

authors	ionic liquid	$N_{Solvents}$	H2 chemical shift regression	R^2
Headley et al.[22]	$EeimPF_6$[a]	7	9.95 − 2.29SPP + 2.26SB − 0.63SA	0.96
Headley et al.[18]	$BmimPF_6$	6	9.37 − 1.61SPP + 2.08SB − 0.56SA	0.93
Lin et al.[20]	$EmimPF_6$	5	9.61 − 1.23SPP + 0.29SB + 0.20SA	0.78

[a] 1,3-Diethylimidazoium hexafluorophosphate.

EmimBr is the only ionic liquid species whose H2 is predicted downfield by the polarity of the medium.

(c) NMR Evidence of Hydrogen Bonding in Ionic Liquids. Both experimental and theoretical NMR data agree with the existence of specific donor−acceptor interactions between counterions in 1-alkyl-3-methylimidazolium salts. The NMR results by Holbrey and Seddon[15] of no significant changes in the H2 chemical shifts of $C_n$mimBF_4 compounds in propanone-d_6 may be attributed to the weak effect of the alkyl chain in the freely dissolved cations, although there is controversy about the anion dependence of the strength of the hydrogen bond between counterions, as it was discussed above in sections 3.1 and 3.2. The experimental NMR studies by Headley et al.[18,22] provided evidence that ionic liquids with BF_4^- present weaker solute−solvent interactions than those with PF_6, which was ascribed to a stronger C2−H···F hydrogen bond. The energies, geometries, and frequencies of ionic liquid structures obtained here by quantum-chemical calculations agree with this conclusion of a more effective interaction between the imidazolium cation and BF_4^- than between the imidazolium cation and PF_6^-.

4. Conclusions

We have presented a computational approach based on quantum-chemical methods to predict, for the first time, reliable ^{1}H and ^{13}C NMR parameters of a series of 1-alkyl-3-methylimidazolium ionic liquids. As a result, calculations have been used as a valuable tool to aid in the interpretation of the experimental NMR data in References and Notes. Thus, we find computational evidence of the existence of a chemical equilibrium between freely separated ions and ion-pair species of ionic liquids in different molecular environments. Calculations indicate that high-polar media or the presence of solvent molecules capable of forming hydrogen bonds favor the formation of solvent-separated ionic structures. Additionally, present study reveals different solvent effects on the NMR chemical shifts of ionic liquids depending upon the nature of solvent−solute interactions. Thus, cluster models to simulate specific interactions between ionic liquids and solvent molecules predict an increasing ^{1}H chemical shift of the H2 atom, whereas the PCM of nonspecific polarization effects of the solvent cage provides the opposite effect in this NMR parameter. Finally, theoretical results are consistent with the existence of hydrogen-bond interactions between the acidic groups of the cation (C2−H2 and alkyl chains) and the nucleophilic atoms of the anion. The strength of such interactions is suggested by calculation to be a sum of attractive electrostatic forces between the donor and acceptor groups and the repulsive steric effects.

A quantum-chemical tool has been developed on the basis of current results of mixed molecular models of ionic liquids—separated ions and ion-paired structures—simulated in different environments (gas-phase model, discrete model, and PCM), which may provide suitable applications in the analysis of ionic liquid behavior in terms of structure−property relationships.

Acknowledgment. We are very grateful to Centro de Computación Científica de la Universidad Autónoma de Madrid for computational facilities.

References and Notes

(1) Improta, R.; Barone, V. *Chem. Rev.* **2004**, *104*, 1231−1254.
(2) Tolman, J. R.; Ruan, K. *Chem. Rev.* **2006**, *106*, 1720−1736.
(3) Tomasi, J.; Mennucci, B.; Cammi, R. *Chem. Rev.* **2005**, *105*, 2999−3094.
(4) Welton, T. *Chem. Rev.* **1999**, *99*, 2071−2083.
(5) Sheldon, K. R. *Chem. Commun.* **2001**, *23*, 2399−2407.
(6) Wasserscheid, P.; Welton, T. *Ionic Liquids in Synthesis*; Wiley−VCH: Weinheim, Germany, 2003.
(7) Rogers, R. D.; Seddon, K. R. *Ionic Liquids as Green Solvents*; ACS Symposium Series 856; American Chemical Society: Washington, DC, 2003.
(8) Dupont, J.; Souza, R. F.; Suarez, P. A. Z. *Chem. Rev.* **2002**, *102*, 3561−3667.
(9) Hussey, U. *Pure Appl. Chem.* **1998**, *60*, 1763−1772.
(10) Rogers, R. D.; Seddon, K. R. *Ionic Liquids IIIB: Fundamentals, Properties, Challenges and Opportunities*; ACS Symposium Series 902; American Chemical Society: Washington, DC, 2005.
(11) Avent, A. G.; Chaloner, P. A.; Day, M. P.; Seddon, K. R.; Welton, T. *Proc. Int. Symp. Molten Salts, 8th* **1992**, *92*−*16*, 98−133.
(12) Bonhôte, P.; Dias, A.; Papageorgiou, N.; Kalyanasundaram, K.; Grätzel, M. *Inorg. Chem.* **1996**, *35*, 1168−1178.
(13) Carda-Broch, S.; Berthod, A.; Asmstrong, D. W. *Anal. Bioanal. Chem.* **2003**, *375*, 191−199.
(14) Suarez, P. A. Z.; Einloft, S.; Dullius, J. E. L.; De Souza, R. F.; Dupont, J. *J. Chim. Phys. Phys.*−*Chim. Biol.* **1998**, *95*, 1626−1639.
(15) Holbrey, J. D.; Seddon, K. R. *J. Chem. Soc., Dalton Trans.* **1999**, 2133−2139.
(16) Seddon, K. R.; Stark, A.; Torres, M.-J. *Pure Appl. Chem.* **2000**, *12*, 2275−2287.
(17) Huang, J.; Chen, P.; Sun, I.; Wang, S. P. *Inorg. Chim. Acta* **2001**, *320*, 7−11.
(18) Headley, A. D.; Jackson, N. M. *J. Phys. Org. Chem.* **2002**, *15*, 52−55.
(19) Mele, A.; Tran, C. D.; De Paoli, S. H. *Angew. Chem.* **2003**, *115*, 4500−4502.
(20) Lin, S.; Ding, M.; Chang, C.; Lue, S. *Tetrahedron* **2004**, *60*, 9441−9446.
(21) Tubbs, J. D.; Hoffman, M. M. *J. Solution Chem.* **2004**, *33* (4), 381−394.
(22) Headley, A. D.; Kotti, S. R. S. S.; Nam, J.; Li, K. *J. Phys. Org. Chem.* **2005**, *18*, 1018−1022.
(23) Consorti, C. S.; Suarez, P. A. Z.; De Souza, R. F.; Burrow, R. A.; Farrar, D. H.; Lough, A. J.; Loh, W.; Da Silva, L. H. M.; Dupont, J. *J. Phys. Chem. B* **2005**, *109*, 4341−4349.
(24) Mele, A.; Romano, G.; Giannone, M.; Ragg, E.; Fronza, G.; Raos, G.; Marcon, V. *Angew. Chem., Int. Ed.* **2006**, *45*, 1123−1126.
(25) Dupont, J.; Suarez, P. A. Z.; De Souza, R. F.; Burrow, R. A.; Kintzinger, J. *Chem.*−*Eur. J.* **2006**, *6*, 2377−2381.
(26) Juergen, J. H.; Mertens, D.; Doelle, A.; Wasserscheid, P.; Carper, W. R. *ChemPhysChem* **2003**, *4* (6), 588−594.
(27) Heimer, N. E.; Del Sesto, R. E.; Carper, W. R. *Magn. Reson. Chem.* **2004**, *42*, 71−75.
(28) Antony, J.; Mertens, D.; Breitenstein, T.; Doelle, A.; Wasserscheid, P.; Carper, W. R. *Pure Appl. Chem*. **2004**, *76* (1), 255−261.
(29) Carper, W. R.; Wahlbeck, P. G.; Antony, J. H.; Mertens, D.; Doelle, A.; Wasserscheid, P *Anal. Bioanal. Chem.* **2004**, *378* (6), 1548−1554.
(30) Carper, W. R.; Wahlbeck, P. G.; Doelle, A. *J. Phys. Chem. A* **2004**, *108* (29), 6096−6099.
(31) Juergen, J. H.; Doelle, A.; Mertens, D.; Wasserscheid, P.; Carper, W. R.; Wahlbeck, P. G. *J. Phys. Chem. A* **2005**, *109* (30), 6676−6682.
(32) Heimer, N. H.; Wilkes, J. S.; Wahlbeck, P. G.; Carper, W. R. *J. Phys. Chem. A* **2006**, *110* (3), 868−874.
(33) Giernoth, R.; Bankmann, D.; Schlörer, N. *Green Chem.* **2005**, *7*, 279−282.
(34) Giernoth, R.; Bankmann, D. *Eur. J. Org. Chem.* **2005**, 4529−4532.
(35) Katsyuba, S. A.; Dyson, P. J.; Vandyukova, E. E.; Chernova, A. V.; Vidis, A. *Helv. Chim. Acta* **2004**, *87*, 2556−2565.
(36) Berg, R. W.; Deetlefs, M.; Seddon, K. R.; Shim, I.; Thompson, J. M. *J. Phys. Chem. B* **2005**, *109*, 19018−19025.
(37) Talaty, E. R.; Raja, S.; Storhaug, V. J.; Doelle, A.; Harper, C. W. *J. Phys. Chem. B* **2004**, *108*, 13177−13184.
(38) Tsuzuki, S.; Tokuda, H.; Hayamizu, K.; Watanabe, M. *J. Phys. Chem. B* **2005**, *109*, 16474−16481.
(39) Gutowski, K. E.; Holbrey, J. D.; Rogers, R. D.; Dixon, D. A. *J. Phys. Chem. A* **2005**, *109*, 23196−23208.
(40) Meng, Z.; Dölle, A.; Carper, W. R. *J. Mol. Struct.* **2002**, *585*, 119−128.
(41) Turner, E. A.; Pye, C. C.; Singer, R. D. *J. Phys. Chem. A* **2003**, *107*, 2277.
(42) Hunt, P. A.; Gould, I. R. *J. Phys. Chem. A* **2006**, *110*, 2269−2282.
(43) Cramer, C. J.; Truhlar, D. G. *Chem. Rev.* **1999**, *99*, 2161−2200.
(44) Crescenzi, O.; Pavone, M.; De Angelis, F.; Barone, V. *J. Phys. Chem. B* **2005**, *109*, 445−453.
(45) Rablen, P. R.; Pearlman, S. A.; Finkbiner, J. *J. Phys. Chem. A* **1999**, *103*, 7357−7363.
(46) Palomar, J.; Dalal, N. S. *J. Phys. Chem. B* **2002**, *106*, 4799−4805.
(47) Dalal, N. S.; Pierce, K. L.; Palomar, J.; Fu, R. *J. Phys. Chem. A* **2003**, *107*, 3471 −3475.
(48) Becke, A. D. *J. Chem. Phys.* **1993**, *98*, 5648.

(49) Lee, C.; Yang, W.; Parr, R. G. *Phys. Rev.* **1988**, *B*37, 785.

(50) Frisch, M. J.; Trucks, G. W.; Schlegel, H. B.; Scuseria, G. E.; Robb, M. A.; Cheeseman, J. R.; Montgomery, J. A., Jr.; Vreven, T.; Kudin, K. N.; Burant, J. C.; Millam, J. M.; Iyengar, S. S.; Tomasi, J.; Barone, V.; Mennucci, B.; Cossi, M.; Scalmani, G.; Rega, N.; Petersson, G. A.; Nakatsuji, H.; Hada, M.; Ehara, M.; Toyota, K.; Fukuda, R.; Hasegawa, J.; Ishida, M.; Nakajima, T.; Honda, Y.; Kitao, O.; Nakai, H.; Klene, M.; Li, X.; Knox, J. E.; Hratchian, H. P.; Cross, J. B.; Bakken, V.; Adamo, C.; Jaramillo, J.; Gomperts, R.; Stratmann, R. E.; Yazyev, O.; Austin, A. J.; Cammi, R.; Pomelli, C.; Ochterski, J. W.; Ayala, P. Y.; Morokuma, K.; Voth, G. A.; Salvador, P.; Dannenberg, J. J.; Zakrzewski, V. G.; Dapprich, S.; Daniels, A. D.; Strain, M. C.; Farkas, O.; Malick, D. K.; Rabuck, A. D.; Raghavachari, K.; Foresman, J. B.; Ortiz, J. V.; Cui, Q.; Baboul, A. G.; Clifford, S.; Cioslowski, J.; Stefanov, B. B.; Liu, G.; Liashenko, A.; Piskorz, P.; Komaromi, I.; Martin, R. L.; Fox, D. J.; Keith, T.; Al-Laham, M. A.; Peng, C. Y.; Nanayakkara, A.; Challacombe, M.; Gill, P. M. W.; Johnson, B.; Chen, W.; Wong, M. W.; Gonzalez, C.; Pople, J. A. *Gaussian 03*, revision C.02; Gaussian, Inc.: Wallingford, CT, 2004.

(51) Miertus, S.; Scrocco, E.; Tomasi, J. *Phys. Chem.* **1981**, *55*, 117.

(52) Cossi, M.; Scalmani, G.; Rega, N.; Barone, V. *J. Chem. Phys.* **2002**, *117*, 43.

(53) Wolinski, K.; Hilton, J. F.; Pulay, P. *J. Am. Chem. Soc.* **1990**, *112*, 8251.

(54) Dietchfield, R. *Mol. Phys.* **1974**, *27*, 789.

(55) Wakai, C.; Oleinikova, A.; Weingärtner, H. *J. Phys. Chem. B* **2005**, *109*, 17028−17030.

(56) Catalán, J.; Lopez, V.; Pérez, P.; Martín-Villamil, R.; Rodríguez, J.-G. *Liebigs Ann.* **1995**, 241−252.

(57) Catalán, J.; Díaz, C.; López, B.; Pérez, P.; DePaz, J.-L. G.; Rodriguez, J.-G. *Liebigs Ann.* **1996**, 1785−1794.

(58) Catalán, J.; Díaz, C. *Liebigs Ann./Recl.* **1997**, 1941−1949.

(59) Elaiwi, A.; Hitchcock, P. B.; Seddon, K. R.; Srinivasan, N.; Hitchcock, P. B.; Seddon, K. R.; Srinivasan, N.; Tan, Y. M.; Welton, T.; Zora, J. A. *J. Chem. Soc., Dalton Trans.* **1995**, 3467.